

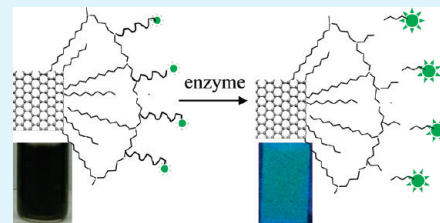
# Peptide-Functionalized Colloidal Graphene via Interdigitated Bilayer Coating and Fluorescence Turn-on Detection of Enzyme

Susanta Kumar Bhunia and Nikhil R. Jana\*

Centre for Advanced Materials, Indian Association for the Cultivation of Science, Kolkata 700032, India

Supporting Information

**ABSTRACT:** Synthesis of colloidal functional graphene is challenging because graphene is water-insoluble and its relatively inert surface made the functionalization a difficult task. Here we report interdigitated bilayer type coating that provide both colloidal stability and functionalization option for graphene. Colloidal graphene oxide is first converted into interdigitated bilayer coated graphene oxide and next they are transformed into colloidal graphene by hydrazine reduction. These coated graphenes can be further transformed into colloidal functional graphene using covalent conjugation chemistry. Functional graphene has been synthesized for optical detection of enzyme where a fluorescent dye is covalently linked through a peptide so that the dye fluorescence is quenched by graphene but switches on once enzymes cleave the peptide bond. The interdigitated bilayer coating reported here is unique as it provides coating thickness <3 nm, offering optically responsive graphene–fluorophore substrate with high colloidal stability.



**KEYWORDS:** graphene, colloid, peptide, polymer coating, enzyme detection, functionalization

## 1. INTRODUCTION

Since the discovery of graphene in 2004,<sup>1</sup> its unique property has been utilized for different electrical and optical detection applications.<sup>2–10</sup> In the electrochemical approach, analyte-induced change in conductance/resistance of graphene or electrochemical response from graphene based electrode platforms have been exploited for detection applications.<sup>2–4</sup> In optical detection approach the strong fluorescence quenching property of fluorophore by graphene/graphene oxide surface has been used for fluorescence-based detection of target DNA/protein.<sup>5–10</sup> One major challenge in those detections is to prepare functional graphene based substrate with high solubility and colloidal stability.<sup>11–13</sup> Soluble functional graphenes are preferred so that the functional/affinity molecules attached on their surface are easily accessible and recognized by analytes. Common functionalization approach involves electrostatic/physical adsorption of affinity molecules on the graphene/graphene oxide surface.<sup>5–10</sup> However, those approaches do not provide robust functionalization and the functional molecules can be easily detached by other molecules present in the environment and functional graphenes often encompass colloidal stability problem. In optical sensor design, the distance between fluorophore and graphene surface should be optimum (typically <5 nm),<sup>14,15</sup> so that quenching via different radiative/nonradiative channels can be efficient but the fluorescence should turn-on once the target analyte recognizes the affinity molecule.<sup>5–10</sup>

Conversion of colloidal graphene oxide, prepared by Hummer's method, via chemical reduction approach is most widely used for large scale synthesis of colloidal graphene and functional graphene.<sup>16</sup> As graphenes produced by this approach have poor colloidal stability, different surface passivation approaches have been developed that includes polymer,<sup>17,18</sup> surfactant,<sup>19</sup> DNA,<sup>20</sup>

aromatic molecules,<sup>21</sup> and covalent conjugation with small molecules<sup>22,23</sup> or polymers.<sup>24,25</sup> Although these coating approaches can produce soluble graphene, their transformation into soluble functional graphene are hardly attempted either because of the absence of chemical functionality useful for conjugation or because of the poor colloidal stability of graphene during conjugation chemistry. We have developed different coating chemistries for nanoparticles that provide colloidal stability in adverse conditions and offer various functionalization options, and they have been extended to different nanoparticles such as gold nanorod, quantum dot, doped semiconductor, metal and metal oxides.<sup>26,27</sup> Recently, we have extended polyacrylate-based coating to colloidal graphene oxide and graphene.<sup>28</sup> Although this coating is useful for synthesis of colloidal functional graphene, the coating is relatively thick (5–10 nm) and nonuniform. Such thick coating produces graphene–fluorophore-based substrate which is poorly optically responsive because of the large separation distance between graphene and fluorophore. Here, we report interdigitated bilayer type coating strategy for graphene/graphene oxide that provide coating thickness <3 nm, producing soluble graphene with high colloidal stability and open options to derive highly optically responsive graphene–fluorophore substrate.

## 2. EXPERIMENTAL SECTION

**Materials and Reagents.** Graphite powder (<20  $\mu\text{m}$ ), didodecyl-dimethylammonium bromide (DDAB) (98%), poly(maleic anhydride-1-octadecene) ( $M_n$  30 000–50 000), O,O'-bis(2-amino propyl)

**Received:** April 11, 2011

**Accepted:** August 11, 2011

**Published:** August 11, 2011

polypropylene glycol-block-polyethylene glycol-block-polypropylene glycol (Product No. 14526,  $M_n$  600), hydrazine hydrate (98%), 4-maleimido butyric acid N-succinimide ester,  $\alpha$ -chymotrypsin from bovine pancreas (Product C3142, MW 25,000), bovine serum albumin (BSA, 98%), trypsin (Product T1426), fluorescamine, fluorescein isothiocyanate (FITC), and Dulbecco's Modified Eagle's Medium (DMEM) were purchased from Sigma Aldrich and used as received. FITC linked peptide FITC-Gly-Gly-Trp-Gly-Cys (MW 792.8, purity >90%) was purchased from GenPro Biotech.

**Instrumentation.** Emission spectra and enzyme assay were performed using Synergy<sup>TM</sup> MX Multi-Mode Microplate Reader. For the quantum yield (QY) measurement, the peptide functionalized G solution was prepared in phosphate buffer of pH 9 and fluorescence was measured at 450 nm excitation. The concentration of fluorescein in the peptide functionalized graphene was determined by measuring the difference in absorbance at 500 nm measured at pH 9 and pH 5 (as shown in Figure S5 in the Supporting Information).

Time correlation single photon counting (TCSPC) measurements were performed with Horiba Jobin Yvon IBH Fluorocube instruments after exciting 440 nm picosecond diode laser (IBH NanoLED). The fluorescence decay was collected using Hamamatsu MCP (R3809) photomultiplier tube and fluorescence decay was analyzed using IBH DAS6 software. A 500  $\mu$ L of peptide functionalized graphene solution was diluted with phosphate buffer solution of pH 8.5 and used for TCSPC measurement.

FTIR study was performed using NICOLET 6700 FT-IR spectroscopy after making pellet with solid KBr. Transmission electron microscopic (TEM) samples were prepared by putting a drop of particle dispersion on carbon coated copper grid and observed with FEI Tecnai G2 F20 microscope. Diluted sample solution was deposited on mica disk and then AFM was measured using VEECO DICP II autoprobe (model AP 0100). Agiltron R3000 Raman spectrometer was used to obtain Raman spectra with 785 nm excitation laser. Bright-field and fluorescence imaging of cells were performed using Olympus microscope IX81 with DP72 digital camera.

**Preparation of Graphene Oxide (GO).** Graphene oxide was prepared by modified Hummer's method. In a beaker 200 mg graphite powder, 100 mg sodium nitrate and  $\sim$ 5 mL concentrated  $H_2SO_4$  was mixed and cooled to 0  $^\circ C$ . Next, 600 mg  $KMnO_4$  was added in a stepwise manner to the cooled solution under vigorous stirring condition so that the temperature should not exceed 20  $^\circ C$ . After the complete addition, temperature of the solution is raised to 35  $^\circ C$  and kept there for 30 min. Next, 10 mL of water was added to the brownish gray paste and the temperature of the solution rose to 98  $^\circ C$ . This temperature was maintained for 15 min and then whole solution then mixed with 28 mL warm water to dilute it further. Next, 500  $\mu$ L 3%  $H_2O_2$  added to reduce the residual permanganate. The suspension turned light yellow cake. This was washed with warm water thoroughly for 7–8 times. The solid was air-dried and dissolved in distilled water by 30 min sonication. Then it was centrifuged at 3000 rpm for 30 min to remove large particles. The supernatant obtained is used as dispersion of GO.

**Preparation of Polymer-Coated Graphene Oxide (GO) and Graphene (G).** Ten mg didodecyl dimethyl ammonium bromide (DDAB) was added to 5 mL of as prepared GO and sonicated for 7 min. After that pH was adjusted to 8 by adding  $\sim$ 75 mg of  $Na_2HPO_4$  followed by 5 min sonication. Next, 3 mL of  $CHCl_3$  was added, stirred for few seconds and kept untouched for phase separation. Colorless  $CHCl_3$  phase becomes brown leaving the colorless aqueous phase, suggesting that GO was transferred from aqueous to organic phase. The bottom organic phase was collected and mixed with  $CHCl_3$  solution of polymaleic anhydride-alt-1-octadecene (40 mg dissolved in 0.5 mL  $CHCl_3$ ) and sonicated for 5 min. Next, a  $CHCl_3$  solution of diamine (*O,O'*-bis(2-aminopropyl)polypropylene glycol-block-polyethylene glycol-block-polypropylene glycol) (60  $\mu$ L dissolved in 500  $\mu$ L  $CHCl_3$ ) was added in two steps. First,  $\sim$ 100  $\mu$ L of diamine solution was added and

sonicated for 1 min. The rest of the diamine solution was added after 20 min. After overnight, the  $CHCl_3$  was evaporated and brownish precipitate was mixed with 3 mL of water and 5 mg of  $Na_2CO_3$ . The whole mixture was sonicated for 5–10 min and left overnight. Optically clear brown solution was obtained, which was used as stock solution.

The polymer-coated GO was further purified from free polymer using acetone induced precipitation of GO. Typically, 1.0 mL of the polymer coated GO solution is mixed with 1.0 mL of acetone and centrifuged at 7000 rpm for 1 min. A brown precipitate was formed, leaving the colorless supernatant. The brown precipitate was collected and dissolved in 200  $\mu$ L of  $H_2O$ . Next, 600  $\mu$ L acetone was added and again centrifuged at 10000 rpm for 2 min. Brown precipitate was collected, dissolved in 2.5 mL of  $H_2O$  and used for further experiments.

Polymer coated GO was converted into polymer coated G via hydrazine-based reduction. Typically, 40  $\mu$ L of hydrazine hydrate was added to the 2.5 mL solution of polymer-coated GO and heated to 70–80  $^\circ C$  for 1 h. A deep black solution appeared. The solution was dialyzed for overnight to remove excess hydrazine.

**Fluorescamine Test.** Fluorescamine test was performed to determine the presence of primary amine in the polymer-coated G. 50  $\mu$ L of polymer-coated G solution was diluted with 300  $\mu$ L of borate buffer solution (pH 9) and then mixed with 50  $\mu$ L of acetone solution of fluorescamine (1 mM). The intense blue-green emission appears almost immediately, suggesting the presence of primary amine. The fluorescence was measured using 400 nm excitation (see Figure S2 in the Supporting Information).

**FITC Functionalization of Polymer-Coated Graphene (G).** One milliliter of dialyzed G solution was mixed with 200  $\mu$ L of phosphate buffer (pH  $\sim$ 8.5) and to it was added a solution of FITC (1.0 mg dissolved in 100  $\mu$ L DMF); the mixture was kept overnight followed by overnight dialysis to remove unbound FITC.

**Peptide Functionalization of Polymer-Coated Graphene (G).** One milliliter of dialyzed G solution was mixed with 200  $\mu$ L phosphate buffer (pH $\sim$ 8.5) and to it a 25  $\mu$ L solution of 4-maleimido-butyric acid N-hydroxy succinimide ester (1.4 mg dissolved in 100  $\mu$ L DMF) was added. After 15 min 100  $\mu$ L of the peptide-FITC solution (1.3 mg dissolved in 200  $\mu$ L DMF) was added to it. Then the mixture was kept at 4  $^\circ C$  for 6 h followed by overnight dialysis to remove excess peptide-FITC and maleimide reagent.

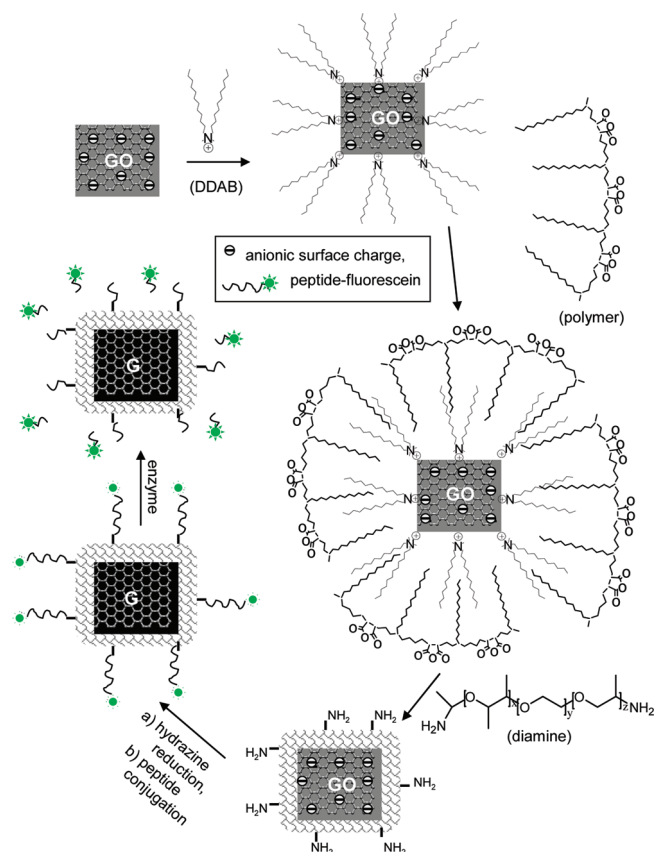
**Enzyme Assay.** Different concentration of  $\alpha$ -chymotrypsin was added to each 50  $\mu$ L of peptide functionalized graphene (G) solution. The total volume of each solution was filled up to 400  $\mu$ L by adding phosphate buffer (pH $\sim$ 8.5) and kept at room temperature. Fluorescence of this solution was measured after 1–6 h using 450 nm excitations. Control experiment with trypsin and BSA experiment was also performed using similar experimental condition. Trypsin experiment was performed to test the enzyme selectivity and BSA experiment was done to check if nonspecific interaction by protein causes fluorescence switching.

**Cellular Enzyme Assay.** H9C2 cells were used for cellular imaging and enzyme assay. First, cells were grown in tissue cultured flask and then subculture in 24-well plates with 0.5 mL of DMEM cell culture media in each plate. For cellular imaging 100  $\mu$ L FITC functionalized graphene was mixed in the cell culture media and incubated for 2 h. Next, cells were washed with media to remove unbound graphenes and then imaged under fluorescence microscope using blue excitation.

For enzyme assay, 100  $\mu$ L of peptide functionalized graphene (G) solution was mixed with 100  $\mu$ L of the cell culture media and kept in  $CO_2$  incubator. Fluorescence was then measured in different time intervals using 450 nm excitation.

### 3. RESULTS AND DISCUSSION

**3.1. Interdigitated Bilayer Coating.** The synthesis approach is shown in Scheme 1. First, colloidal graphene oxide is extracted

Scheme 1. Coating and Functionalization Strategy of Colloidal Graphene Oxide (GO) and Graphene (G)<sup>a</sup>

<sup>a</sup> Fluorescence of G bound fluorophore is quenched but switches on by enzyme action. GO is first coated with DDAB to make it hydrophobic. Next, polymer is attached to GO via interdigitated bilayer structure. Finally, diamine is reacted with anhydride groups of polymer to derive amine terminated coating. Acid groups are formed in coating backbone during the reaction of amine with anhydride, which is not shown for clarity.

into organic solvent after electrostatic binding with didodecylmethyl ammonium bromide (DDAB).<sup>19</sup> Hydrophobic graphene oxide is then converted into water-soluble polymer coated graphene oxide via coating with amphiphilic polymer poly(maleic anhydride-1-octadecene) followed by diamine linking.<sup>29,30</sup> Hydrazine reduction converts graphene oxide into graphene without any loss of solubility. Water-soluble colloidal graphene is then transformed into peptide-functionalized colloidal graphene using conjugation chemistry.

The coating combines two very efficient steps: the solvent extraction/phase transfer of graphene oxide by DDAB capping<sup>19</sup> and amphiphilic polymer coating of DDAB capped hydrophobic graphene oxide -- a coating strategy that is well-established for variety of hydrophobic nanoparticles.<sup>26,29,30</sup> The DDAB capping induce efficient solvent extraction via formation of ion associates with anionic graphene oxide as well as offers the hydrophobic anchoring of amphiphilic polymer via interdigitated bilayer structure (shown in Scheme 1). The thickness of this coating is limited by the bilayer thickness but its hydrophobic nature protects the core graphene from aggregation and outer polar groups offer water solubility. After the polymer coating, the diamines are reacted with anhydride groups present in polymer. It is well-known that

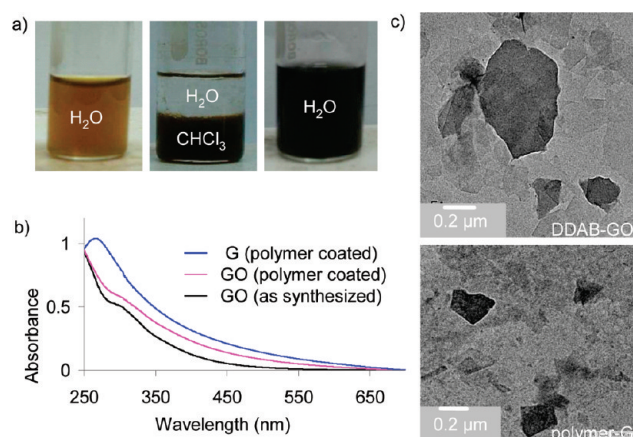


**Figure 1.** (a) Digital image of colloidal solution of as synthesized graphene oxide (GO) (left), phase transfer of aqueous GO into chloroform using DDAB (middle) and aqueous solution of polymer coated graphene (G) (right). (b) UV-visible absorption spectra of as synthesized GO and polymer-coated GO/G. (c) TEM images of DDAB capped GO and polymer-coated G.

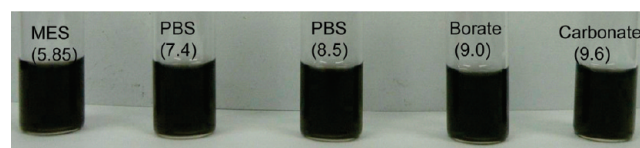


**Figure 2.** Stable colloidal solution of polymer coated graphene in different buffer media.

primary amine group reacts with anhydride, forming amide bond along with the creation of carboxylic acid group. We have added diamine in two steps so that first they are present in low concentration and help cross-linking the polymer via reaction with both the amine groups.<sup>26</sup> In latter stage when diamines becomes equivalent to anhydride, one amine group reacts with anhydride and the other unreacted one is available for conjugation chemistry.

This type polymer coating is first developed by Parak et al<sup>29</sup> and since then widely used for coating of variety of hydrophobic nanoparticle, in transforming into water-soluble nanoparticle.<sup>30,31</sup> The established mechanism is that long chain octadecene groups of polymer are incorporated into the hydrophobic groups around nanoparticle, (as shown in Scheme 1) forming interdigitated bilayer structures. In present case the first layer consist of DDAB and second layer consists of polymer. The polar groups of polymer make the coated particle water-soluble. Similar type of interdigitated bilayer structure is also observed for surfactant-capped nanoparticles such as fatty acid-capped Ag nanoparticle,<sup>32</sup> cetyltrimethylammonium bromide (CTAB)-capped gold nanorod<sup>33</sup> and DDAB capped gold nanospheres.<sup>34</sup> In order to prove the interdigitated bilayer structure in our coating we studied DTA, TGA of coated graphene/graphene oxide (see the Supporting Information) and results are similar to earlier studies.<sup>31,33,34</sup> DTA study shows phase transition at 70–110 °C and melting transition at 180–220 °C. TGA study shows mass loss in 200–300 °C due to DDAB degradation and mass loss at 390–420 °C due to polymer degradation.<sup>31,34</sup> This study supports the presence of both DDAB and polymer as coating materials. The broad temperature range for melting transition indicates that it is associated



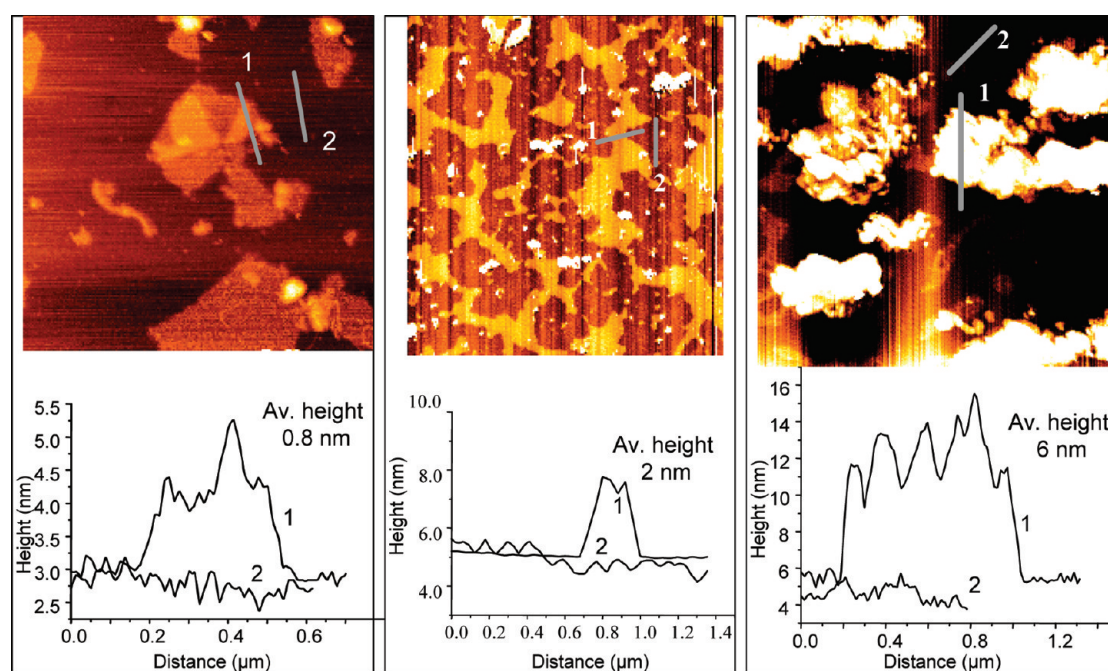


**Figure 3.** AFM height images of as-synthesized graphene oxide (left), DDAB-capped graphene oxide (middle), and polymer-coated graphene (right), showing the thickness of DDAB and polymer coating are  $<1$  and  $<3$  nm, respectively. The thickness of DDAB coating is determined as follows: (height of DDAB capped graphene oxide – height of graphene oxide)/2. Similarly, thickness of polymer coating is determined as follows: (height of polymer coated graphene oxide – height of graphene oxide)/2.

with desorption of DDAB in aggregated forms with the long chain octadecene groups of the polymer as well as the desorption of DDAB from graphene/graphene oxide surface.<sup>31</sup> NMR study of DDAB and polymer coated graphene oxide also supports the coating (see the Supporting Information). Proton NMR study of DDAB coated graphene oxide shows the presence of DDAB and signature of broad signal for protons adjacent to ammonium groups suggesting that ammonium groups are adsorbed on the graphene oxide surface as shown in Scheme 1. NMR of polymer coated graphene oxide shows the signature of DDAB, polymer and diamine (see the Supporting Information) The broad signal of some DDAB protons suggest that they still maintains similar adsorption pattern in polymer coated graphene oxide and corroborates the coating mechanism shown in Scheme 1.

Figure 1 shows the solvent extraction step along with the optical property of graphene oxide/graphene before and after polymer coating. Optical property of colloidal graphene changes significantly compared to colloidal graphene oxide.<sup>35</sup> Although colloidal graphene oxide is brown in color, colloidal graphene appears black with significant enhanced absorption from UV to NIR region with peak at 270 nm. Colloidal stability of graphene produced by this approach is tested in different aqueous buffer medium. Results show that graphene solutions are stable over months. (Figure 2) Polymer coated graphene oxide/graphene has been characterized by TEM, AFM, FTIR, NMR, Raman, and thermogravimetric analysis.

AFM study has been performed after both polymer coating and amine modification to determine tentative thickness of coating (Figure 3). The thickness of polymer coating is determined after subtracting the height of graphene oxide from the height of polymer-coated graphene oxide and then dividing by 2, which comes about 2–3 nm. Similarly, the thickness of the hydrophobic DDAB coating is determined after subtracting the

height of graphene oxide from the height of DDAB capped graphene oxide and then dividing by two, which comes to about 0.6 nm. This study shows that coating thickness of DDAB-capped hydrophobic graphene oxide is  $<1$  nm and polymer coated hydrophilic graphene oxide/graphene is  $<3$  nm. (Figure 3) In order to make a quite reliable estimate of polymer coating thickness the heights of bare graphene oxide, DDAB coated graphene oxide and polymer coated graphene oxide have been measured for different batches and in different areas of deposited film. About 12–15 graphene/graphene oxide heights were measured for each sample and their heights were between 0.7 and 1.0 nm for bare graphene oxide, between 1.8 and 2.2 nm for DDAB coated graphene oxide and between 5.0 and 7.5 nm for polymer coated graphene oxide. This result suggests that increased thickness for DDAB coated graphene oxide and polymer coated graphene oxide as compared to bare graphene oxide are realistic and determined thickness of DDAB and polymer coating are reliable. We have also tested that this polymer coated graphene oxide is not a simple graphene–polymer nanocomposite. In a control experiment, we mixed aqueous graphene oxide solution with chloroform solution of polymer, shaken vigorously until chloroform gets evaporated and finally polymer was hydrolyzed by  $\text{Na}_2\text{CO}_3$ . The graphene–polymer composite thus formed have poor water solubility and completely water insoluble after hydrazine reduction. This result suggests that simple graphene–polymer composite is unable to provide colloidal stability of graphene unless the polymer is coated via interdigitated bilayer. One advantage of this interdigitated bilayer type coating is that coating thickness is dictated by the bilayer thickness. However, in solution, polymers and amines are free to expose outward direction and thus actual distance can be  $>3$  nm. Nevertheless, the thickness is optimum enough for responsive optical detection applications.

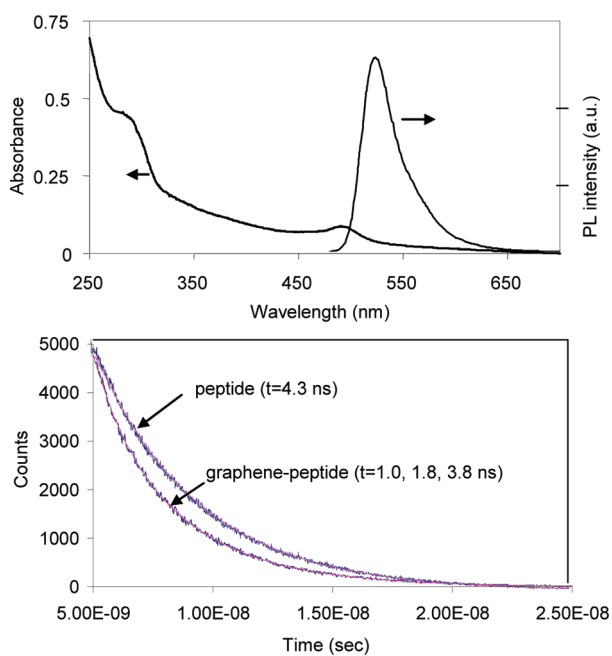


**Figure 4.** (Top) Absorption and fluorescence property of peptide functionalized graphene where fluorescence arises from fluorescein present on peptide backbone. (Bottom) Fluorescence lifetime decay curve (pink line, experimental data; black line, fitting) of fluorescein showing that the single exponential lifetime gets modified into triple exponential life times after attachment with graphene.

**3.2. Functionalization of Graphene via Covalent Conjugation.** The described coating is unique compared to earlier approaches, as it can produce colloiddally stable graphene in milligram scale with the easier scaling up option and opens various functionalization scopes via conjugation chemistry without any loss of colloidal stability. The functionalization can be performed using primary amine present on the coating backbone, the presence of which has been tested by fluorescamine titration. To demonstrate that functionalization can be achieved with the coated graphene, we have synthesized fluorescein and peptide-fluorescein-functionalized colloidal graphene and used them as probes for cellular imaging and enzyme detection, respectively. Fluorescein functionalization was performed by reaction of primary amine present on coated graphene with fluorescein isothiocyanate (FITC). For peptide functionalization, we have selected FITC-Gly-Gly-Trp-Gly-Cys, such that thiol group of Cys is used for covalent linkage with primary amine terminated graphene, FITC component provides fluorescence and Trp site helps the enzyme  $\alpha$ -chymotrypsin to recognize and cleave the peptide. The covalent linking of graphene with peptide is performed using 4-maleimido butyric acid N-succinimide ester-based conjugation, where maleimide group react with Cys thiol group and succinimide group helps to link with primary amine of polymer-coated graphene.

The optical property of functionalized graphene contributes both the absorbance due to graphene and fluorescence due to fluorescein. (Figure 4 and the Supporting Information) However, the fluorescein fluorescence gets quenched by >50% (see the Supporting Information). The lifetime of fluorescein gets modified after bound with graphene with the appearance of shorter components, further suggesting the influence of graphene. Fluorescein functionalization offers visualization of graphene

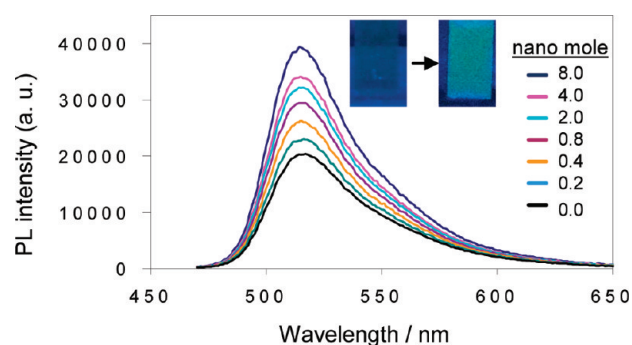


**Figure 5.** Enzyme assay using functional graphene. Different amounts of  $\alpha$ -chymotrypsin are mixed with colloidal solution of peptide-functionalized graphene and fluorescence spectra were measured after 5 h. Inset shows the visible change after 5 h as observed under UV light for 8 nano mole enzyme.

under fluorescence microscope and study of their interaction/internalization by cells (see the Supporting Information). Although fluorescein fluorescence gets quenched significantly, the remaining fluorescence is bright enough to see them under fluorescence microscope. However, a relatively higher dose is required for cellular labeling because of the presence of anionic carboxylate and nonionic PEG functional groups on graphene surface, which are known for lowering cellular interaction.<sup>27</sup> In addition, cellular internalization is low as compared to their adsorption on the cell surface, possibly because of the larger size of graphene. This work demonstrates that various functional graphene can be synthesized from the interdigitated bilayer-coated graphene without significant loss of colloidal stability.

**3.3. Peptide-Functionalized Colloidal Graphene-Based Enzyme Detection.** The peptide-functionalized graphene thus prepared has been used for enzyme detection. Figure 5 shows that peptide functionalized graphene becomes responsive to enzyme and quenched fluorescence returns back in presence of chymotrypsin. The same amount of peptide functionalized graphene was mixed with different amount of chymotrypsin and emission spectra were monitored after 5 h. Results show that the emission intensity of solution mixture increases with the increasing concentration of chymotrypsin with the enzyme detection sensitivity in the nanomolar range. In the higher enzyme concentration range the color change is visible even in naked eye (inset of Figure 5). Control experiments show that this responsive action is specific and does not occur for other enzyme or protein (see the Supporting Information).

To further extend the in vitro application,<sup>36</sup> we mixed this peptide-functionalized graphene probe with cultured cell lines that produce such enzymes and observed the enzyme response. (Figure 6) The graphene probe responds to the enzyme present in culture media/cell and fluorescence turns-on. Imaging study of cells shows that they stay healthy even after 18 h (see the Supporting Information). However, no significant fluorescence was observed from cells possibly because fluorescein gets detached from graphene by enzyme action. This study further suggests that functional graphene has low cytotoxicity and can be used for cellular assay of enzymes. Functionalized graphene used here is very robust because peptide is covalently linked with coated graphene and gives detection advantage in complex in vitro conditions.

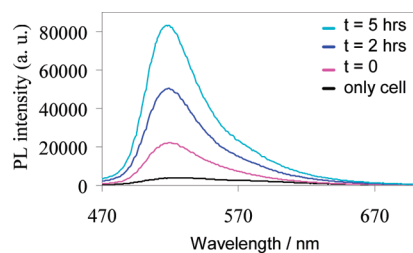


**Figure 6.** Cellular enzyme assay using functional graphene. H9C2 cells along with culture media were mixed with peptide-functionalized graphene solution, incubated for different time and then fluorescence was recorded. Increased fluorescence is due to the enzyme action.

#### 4. CONCLUSION

In conclusion, we have developed an interdigitated bilayer coating in deriving water-soluble functional graphene. The coating thickness is <3 nm and offers covalent functionalization of different affinity molecules. The covalent approach makes the functionalization robust and optimum separation distance offers optically responsive graphene substrate. Using this coating enzyme responsive colloidal functional graphene has been synthesized for in vitro enzyme assay, demonstrating that a variety of other functional graphene can be synthesized.

Although graphene oxide has surface functional groups such as carboxyl, hydroxyl, carbonyl etc., they are very low in density and thus have very limited use for functionalization. In addition, such a functionalization strategy usually does not offer solubilization when graphene oxides are converted into graphene by chemical reduction. Recently reported Diels–Elder reaction of graphene can be an interesting approach for functionalization.<sup>37</sup> However, this approach is yet to be tested for the preparation of various colloidal functional graphene. It is important to note that functionalization of graphene and preparation of soluble functional graphene are two different issue. Although many functionalization methods are reported and they worked well in film based platform, they may not be successful for the preparation of soluble functionalization graphene. This is because solubilization requires solving the colloidal stability problem that depends on the extent of functionalization and nature of functional molecule. In contrast, our polymer coating offers solubilization of graphene and functionalization option via new functional groups, which can be a few hundred to thousands per graphene.<sup>26</sup>

#### ■ ASSOCIATED CONTENT

Supporting Information. Characterization details of coating, control study of enzyme activity. This material is available free of charge via Internet at <http://pubs.acs.org>.

#### ■ AUTHOR INFORMATION

##### Corresponding Author

\*E-mail: [camnrj@iacs.res.in](mailto:camnrj@iacs.res.in). Telephone: +91-33-24734971. Fax: +91-33-24732805.

#### ■ ACKNOWLEDGMENT

The authors thank DST and DBT, government of India, for financial support. S.K.B. acknowledges CSIR, India, for research fellowship.

#### ■ REFERENCES

- Novoselov, K. S.; Geim, A. K.; Morozov, S. V.; Jiang, D.; Zhang, Y.; Dubonos, S. V.; Grigorieva, I. V.; Firsov, A. A. *Science* **2004**, *306*, 666–669.
- Robinson, J. T.; Perkins, F. K.; Snow, E. S.; Wei, Z.; Sheehan, P. E. *Nano Lett.* **2008**, *8*, 3137–3140.
- Koehler, F. M.; Luechinger, N. A.; Ziegler, D.; Athanassiou, E. K.; Grass, R. N.; Rossi, A.; Hierold, C.; Stemmer, A.; Stark, W. J. *Angew. Chem., Int. Ed.* **2009**, *48*, 224–227.
- Dua, V.; Surwade, S. P.; Ammu, S.; Agnihotra, S. R.; Jain, S.; Roberts, K. E.; Park, S.; Ruoff, R. S.; Manohar, S. K. *Angew. Chem., Int. Ed.* **2010**, *49*, 2154–2157.
- Lu, C.-H.; Yang, H.-H.; Zhu, C.-L.; Chen, X.; Chen, G.-N. *Angew. Chem., Int. Ed.* **2009**, *48*, 4785–4787.
- He, S.; Song, B.; Li, D.; Zhu, C.; Qi, W.; Wen, Y.; Wang, L.; Song, S.; Fang, H.; Fan, C. *Adv. Funct. Mater.* **2010**, *20*, 453–459.
- Chang, H.; Tang, L.; Wang, Y.; Jiang, J.; Li, J. *Anal. Chem.* **2010**, *82*, 2341–2346.
- Li, F.; Huang, Y.; Yang, Q.; Zhong, Z.; Li, D.; Wang, L.; Song, S.; Fan, C. *Nanoscale* **2010**, *2*, 1021–1026.
- Loh, K. P.; Bao, Q.; Eda, G.; Chhowalla, M. *Nat. Chem.* **2010**, *2*, 1015–1024.
- Wang, Y.; Li, Z.; Hu, D.; Lin, C.-T.; Li, J.; Lin, Y. *J. Am. Chem. Soc.* **2010**, *132*, 9274–9276.
- Rao, C. N. R.; Sood, A. K.; Subrahmanyam, K. S.; Govindaraj, A. *Angew. Chem., Int. Ed.* **2009**, *48*, 7752–7777.
- Kamat, P. V. *J. Phys. Chem. Lett.* **2010**, *1*, 520–527.
- Park, S.; Ruoff, R. S. *Nat. Nanotechnol.* **2009**, *4*, 217–224.
- Fu, Y.; Lakowicz, J. R. *J. Phys. Chem. B* **2006**, *110*, 22557–22562.
- Pons, T.; Medintz, I. L.; Sapsford, K. E.; Higashiyama, S.; Grimes, A. F.; English, D. S.; Mattoussi, H. *Nano Lett.* **2007**, *7*, 3157–3164.
- Dreyer, D. R.; Park, S.; Bielawski, C. W.; Ruoff, R. S. *Chem. Soc. Rev.* **2010**, *39*, 228–240.
- Stankovich, S.; Piner, R. D.; Chen, X. Q.; Wu, N. Q.; Nguyen, S. T.; Ruoff, R. S. *J. Mater. Chem.* **2006**, *16*, 155–158.
- Choi, E.-Y.; Han, T. H.; Hong, J.; Kim, J. E.; Lee, S. H.; Kim, H. W.; Kim, S. O. *J. Mater. Chem.* **2010**, *20*, 1907–1912.
- Liang, Y.; Wu, D.; Feng, X.; Mullen, K. *Adv. Mater.* **2009**, *21*, 1679–1683.
- Patil, A. J.; Vickery, J. L.; Scott, T. B.; Mann, S. *Adv. Mater.* **2009**, *21*, 3159–3164.
- Su, Q.; Pang, S.; Alijani, V.; Li, C.; Feng, X.; Mullen, K. *Adv. Mater.* **2009**, *21*, 3191–3195.
- Si, Y.; Samulski, E. T. *Nano Lett.* **2008**, *8*, 1679–1682.
- Park, S.; Dikin, D. A.; Nguyen, S. T.; Ruoff, R. S. *J. Phys. Chem. C* **2009**, *113*, 15801–15804.
- Lee, S. H.; Dreyer, D. R.; An, J.; Velamakanni, A.; Piner, R. D.; Park, S.; Zhu, Y.; Kim, S. O.; Bielawski, C. W.; Ruoff, R. S. *Macromol. Rapid Commun.* **2010**, *31*, 281–288.
- Zhang, C.; Yuan, Y.; Zhang, S.; Wang, Y.; Liu, Z. *Angew. Chem., Int. Ed.* **2011**, *50*, 6851–6854.
- Basiruddin, S.; Saha, A.; Pradhan, N.; Jana, N. R. *J. Phys. Chem. C* **2010**, *114*, 11009–11017.
- Jana, N. R. *Phys. Chem. Chem. Phys.* **2011**, *13*, 385–396.
- Saha, A.; Basiruddin, S.; Ray, S. C.; Roy, S. S.; Jana, N. R. *Nanoscale* **2010**, *2*, 2777–2782.
- Pellegrino, T.; Manna, L.; Kudera, S.; Liedl, T.; Koktysh, D.; Rogach, A. L.; Keller, S.; Radler, J.; Natile, G.; Parak, W. J. *Nano Lett.* **2004**, *4*, 703–707.
- Lin, C.-A. J.; Sperling, R. A.; Li, J. K.; Yang, T.-Y.; Li, P.-Y.; Zanella, M.; Chang, W. H.; Parak, W. J. *Small* **2008**, *4*, 334–341.
- Moros, M.; Pelaz, B.; Lopez-Larrubia, P.; Garcia-Martin, M. L.; Grazu, V.; de la Fuente, J. M. *Nanoscale* **2010**, *2*, 1746–1755.
- Patil, V.; Mayya, K. S.; Pradhan, S. D.; Sastry, M. *J. Am. Chem. Soc.* **1997**, *119*, 9281–9282.
- Nikoobakht, B.; El-Sayed, M. A. *Langmuir* **2001**, *17*, 6368–6374.

- (34) Zhang, L.; Sun, X.; Song, Y.; Jiang, X.; Dong, S.; Wang, E. *Langmuir* **2006**, *22*, 2838–2843.
- (35) Li, D.; Muller, M. B.; Gilge, S.; Kaner, R. B.; Wallace, G. G. *Nat. Nanotechnol.* **2008**, *3*, 101–105.
- (36) Moravec, R. A.; O'Brien, M. A.; Daily, W. J.; Scurria, M. A.; Bernad, L.; Riss, T. L. *Anal. Biochem.* **2009**, *387*, 294–302.
- (37) Sarkar, S.; Bekyarova, E.; Niyogi, S.; Haddon, R. C. *J. Am. Chem. Soc.* **2011**, *133*, 3324–3327.